Ca^{2+}-Activated Reactive Oxygen Species Production by *Arabidopsis* RbohH and RbohJ Is Essential for Proper Pollen Tube Tip Growth[W]

Hidetaka Kaya,[a,b] Ryo Nakajima,[a] Megumi Iwano,[c] Masahiro M. Kanaoka,[d,e] Sachie Kimura,[a,1] Seiji Takeda,[f] Tomoko Kawarazaki,[a] Eriko Senzaki,[a] Yuki Hamamura,[d] Tetsuya Higashiyama,[d,e,g] Seiji Takayama,[c] Mitsutomo Abe,[b] and Kazuyuki Kuchitsu[a,2]

[a] Department of Applied Biological Science, Tokyo University of Science, Noda, Chiba 278-8510, Japan
[b] Department of Biological Science, Graduate School of Science, University of Tokyo, Bunkyo-ku, Tokyo 113-0033, Japan
[c] Graduate School of Biological Sciences, Nara Institute of Science and Technology, Ikoma, Nara 630-0101, Japan
[d] Division of Biological Science, Graduate School of Science, Nagoya University, Nagoya, Aichi 464-8602, Japan
[e] Institute of Transformative Bio-Molecules, Nagoya University, Nagoya, Aichi 464-8602, Japan
[f] Graduate School of Life and Environmental Sciences, Kyoto Prefectural University, Soraku-gun, Kyoto 619-0244, Japan
[g] JST, ERATO, Higashiyama Live-Holonics Project, Nagoya University, Nagoya, Aichi 464-8602, Japan

ORCID ID: 0000-0001-8854-0375 (K.K.)

In flowering plants, pollen germinates on the stigma and pollen tubes grow through the style to fertilize the ovules. Enzymatic production of reactive oxygen species (ROS) has been suggested to be involved in pollen tube tip growth. Here, we characterized the function and regulation of the NADPH oxidases RbohH and RbohJ (Respiratory burst oxidase homolog H and J) in pollen tubes in *Arabidopsis thaliana*. In the *rbohH* and *rbohJ* single mutants, pollen tube tip growth was comparable to that of the wild type; however, tip growth was severely impaired in the double mutant. In vivo imaging showed that ROS accumulation in the pollen tube was impaired in the double mutant. Both RbohH and RbohJ, which contain Ca^{2+} binding EF-hand motifs, possessed Ca^{2+}-induced ROS-producing activity and localized at the plasma membrane of the pollen tube tip. Point mutations in the EF-hand motifs impaired Ca^{2+}-induced ROS production and complementation of the double mutant phenotype. We also showed that a protein phosphatase inhibitor enhanced the Ca^{2+}-induced ROS-producing activity of RbohH and RbohJ, suggesting their synergistic activation by protein phosphorylation and Ca^{2+}. Our results suggest that ROS production by RbohH and RbohJ is essential for proper pollen tube tip growth, and furthermore, that Ca^{2+}-induced ROS positive feedback regulation is conserved in the polarized cell growth to shape the long tubular cell.

INTRODUCTION

Plant reproduction starts with the settling of pollen grains on the stigma of the pistil. After the grains germinate, the pollen tubes grow through the transmitting tract of the style and septum and finally reach the ovule, where fertilization occurs. Pollen tubes expand by tip growth, in which the apex of the cell grows faster than the other sides, generating a long tubular structure (Qin and Yang, 2011).

Calcium ions (Ca^{2+}) and various Ca^{2+}-related proteins play central roles in pollen tube tip growth (reviewed in Konrad et al., 2011; Qin and Yang, 2011; Hepler et al., 2012; Steinhorst and Kudla, 2013). For example, Ca^{2+}-permeable channels are known to be expressed in pollen tubes; examples include the stretch-activated Ca^{2+} channel (Dutta and Robinson, 2004), the cyclic

nucleotide-gated channel (Frietsch et al., 2007), glutamate receptor–like channels (Michard et al., 2011), a Ca^{2+} pump (Schiøtt et al., 2004), and Ca^{2+} sensor proteins containing Ca^{2+} binding EF-hand motifs such as calmodulins, calmodulin-like proteins, calcium-dependent protein kinases, and calcineurin B-like proteins (Pina et al., 2005; Zhou et al., 2009). In addition, cytoplasmic Ca^{2+} oscillations and a tip-focused Ca^{2+} gradient are essential for pollen tube growth (Messerli et al., 2000; Feijó et al., 2001; Iwano et al., 2004, 2009; Cárdenas et al., 2008).

In addition to Ca^{2+}, reactive oxygen species (ROS) are essential for proper pollen tube tip growth. ROS accumulate at the growing tip of pollen tubes, while ROS scavengers reduce ROS levels and inhibit pollen tube growth (Potocký et al., 2007, 2012). Diphenylene iodonium (DPI), an inhibitor of NADPH oxidase (NOX), also inhibits ROS accumulation at the tip (Potocký et al., 2007, 2012). These findings suggest that the ROS produced by NOX are involved in pollen tube tip growth. Furthermore, the addition of Ca^{2+} to the pollen tube tip increases ROS accumulation (Potocký et al., 2007, 2012; Wilkins et al., 2011), indicating that Ca^{2+} regulates ROS production during pollen tube tip growth. However, the molecular mechanisms of ROS production and its regulation during pollen tube tip growth remain unknown.

ROS, including superoxide anion radicals, hydroxyl radicals, and hydrogen peroxide, are critical signaling molecules in animals. ROS

produced by NOX are essential to brain physiology, the immune system, the vasculature, the digestive tract, and hormone synthesis (Brown and Griendling, 2009). In plants, ROS produced by NOX are involved in cell growth, development, and responses to abiotic and biotic stresses (reviewed in Suzuki et al., 2011; Marino et al., 2012). *Respiratory burst oxidase homolog* (*Rboh*) genes encode NOX in plants. All plant Rboh proteins possess two EF-hand motifs in the N-terminal intracellular region, six transmembrane helices, and a FAD/NADPH binding domain in the C-terminal intracellular region. The *Arabidopsis thaliana* genome has 10 *Rboh* genes (*RbohA* to *RbohJ*) (Torres and Dangl, 2005). The functions of 4 of these 10 family members have been reported. *RbohB* is involved in seed after-ripening (Müller et al., 2009). Both *RbohD* and *RbohF* are involved in stress responses, such as pathogen defense (Torres et al., 2002) and abscisic acid–induced stomatal closure (Kwak et al., 2003). *RbohF* was recently shown to be involved in Casparian strip formation in roots (Lee et al., 2013). RbohC, also known as *ROOT HAIR DEFECTIVE2* (*RHD2*), is involved in root hair tip growth (Foreman et al., 2003). RbohC/RHD2, RbohD, and RbohF proteins have also been shown to possess ROS-producing activity that is activated by both Ca^{2+} binding to EF-hand motifs and protein phosphorylation by heterologous expression in HEK293T cells (Ogasawara et al., 2008; Takeda et al., 2008; Kimura et al., 2012).

In this study, we characterize the two *Arabidopsis Rboh* genes that are specifically expressed in pollen: *RbohH* and *RbohJ*. The *rbohH rbohJ* double mutant is defective in pollen tube tip growth, suggesting the importance of these genes in pollen tube growth, which is also supported by a recent report (Boisson-Dernier et al., 2013). Furthermore, we show the ROS-producing activities of RbohH and RbohJ and characterize their regulatory mechanisms by Ca^{2+} and protein phosphorylation using a heterologous expression system. We propose that the maintenance of a proper pollen tube tip requires ROS production by RbohH and RbohJ, which are activated by Ca^{2+} via their EF-hand motifs.

RESULTS

RbohH and *RbohJ* Are Expressed in Pollen Grains and Growing Pollen Tubes

Among the 10 Rboh proteins of *Arabidopsis*, RbohH and RbohJ had the highest level of amino acid sequence similarity (80%; Supplemental Figure 1A and Supplemental Data Set 1). According to the *Arabidopsis* eFP Browser microarray database (http://www.bar.utoronto.ca/efp/cgi-bin/efpWeb.cgi; Schmid et al., 2005; Winter et al., 2007), *RbohH* and *RbohJ* are expressed in pollen grains. We examined the tissue-specific expression profiles of *RbohH* and *RbohJ* by RT-PCR. Both genes were expressed in flowers, including inflorescence meristems, but not in 10-d-old seedlings, roots, rosette leaves, or cauline leaves (Figure 1A). We further tested their expression within flowers and found that both genes were expressed in pollen grains (Figure 1B). To examine their spatial expression patterns, we generated transgenic plants harboring *RbohH$_{pro}$:GUS* or *RbohJ$_{pro}$:GUS* in the wild-type Columbia-0 (Col-0) background (Supplemental Figure 2). In both transgenic plants, β-glucuronidase (GUS) staining was detected in pollen grains and pollen tubes but not in the other floral organs

(Figures 1C and 1D). These results indicate that both *RbohH* and *RbohJ* are specifically expressed in pollen grains and pollen tubes.

rbohH rbohJ Double Mutants Are Defective in Pollen Tube Tip Growth and Exhibit Reduced Fertility

To examine the developmental functions of *RbohH* and *RbohJ*, we analyzed T-DNA insertion mutants (Figure 2A). All mutants showed deletions of the genomic DNA fragments associated with T-DNA insertions. Full-length transcripts of *RbohH* or *RbohJ* were not detected in these T-DNA insertion mutants (Figure 2B).

Given that *RbohH* and *RbohJ* are expressed in pollen grains (Figures 1B to 1D), we analyzed the self-fertilization rates in wild-type and mutant plants. When the homozygous *rbohH-3* and *rbohJ-2* single mutants were self-pollinated, the silique length and the average number of seeds per silique were comparable to those of the wild type (Figures 2C, panels 2 and 3, and 2D). However, in the homozygous *rbohH-3 rbohJ-2* double mutant, the silique was shorter than in the wild type (Figure 2C) and there were significantly fewer seeds per silique (Figure 2D). To investigate whether the reduced fertility in *rbohH-3 rbohJ-2* was caused by the pistil, the pollen grains, or both, we cross-pollinated the wild-type and double mutant plants. When the pistils of *rbohH-3 rbohJ-2* were pollinated with wild-type pollen grains, silique length and average number of seeds were not affected (Figures 2C and 2D). Conversely, when the wild-type pistils were pollinated with the pollen grains of the double mutant, the siliques were shorter (Figure 2C) and contained significantly fewer
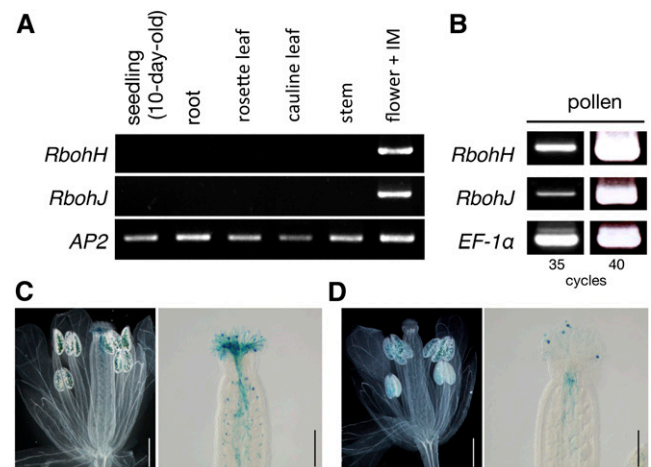

Figure 1. *RbohH* and *RbohJ* Genes Were Expressed in Pollen Grains.

(A) RT-PCR analysis of *RbohH* and *RbohJ* expression in different tissues. IM, inflorescence meristem. *APETALA2* (*AP2*) was used as a control. Two biological and technical replicates were performed.
(B) RT-PCR analysis of *RbohH* and *RbohJ* expression in pollen grains. Total RNA was extracted from pollen grains. *ELONGATION FACTOR-1α* (*EF-1α*) was used as a control. Two biological and technical replicates were performed.
(C) and **(D)** GUS staining of an opened flower and pistil of *RbohH$_{pro}$:GUS* **(C)** or *RbohJ$_{pro}$:GUS* **(D)**. Bars = 500 μm (left panels) and 200 μm (right panels).
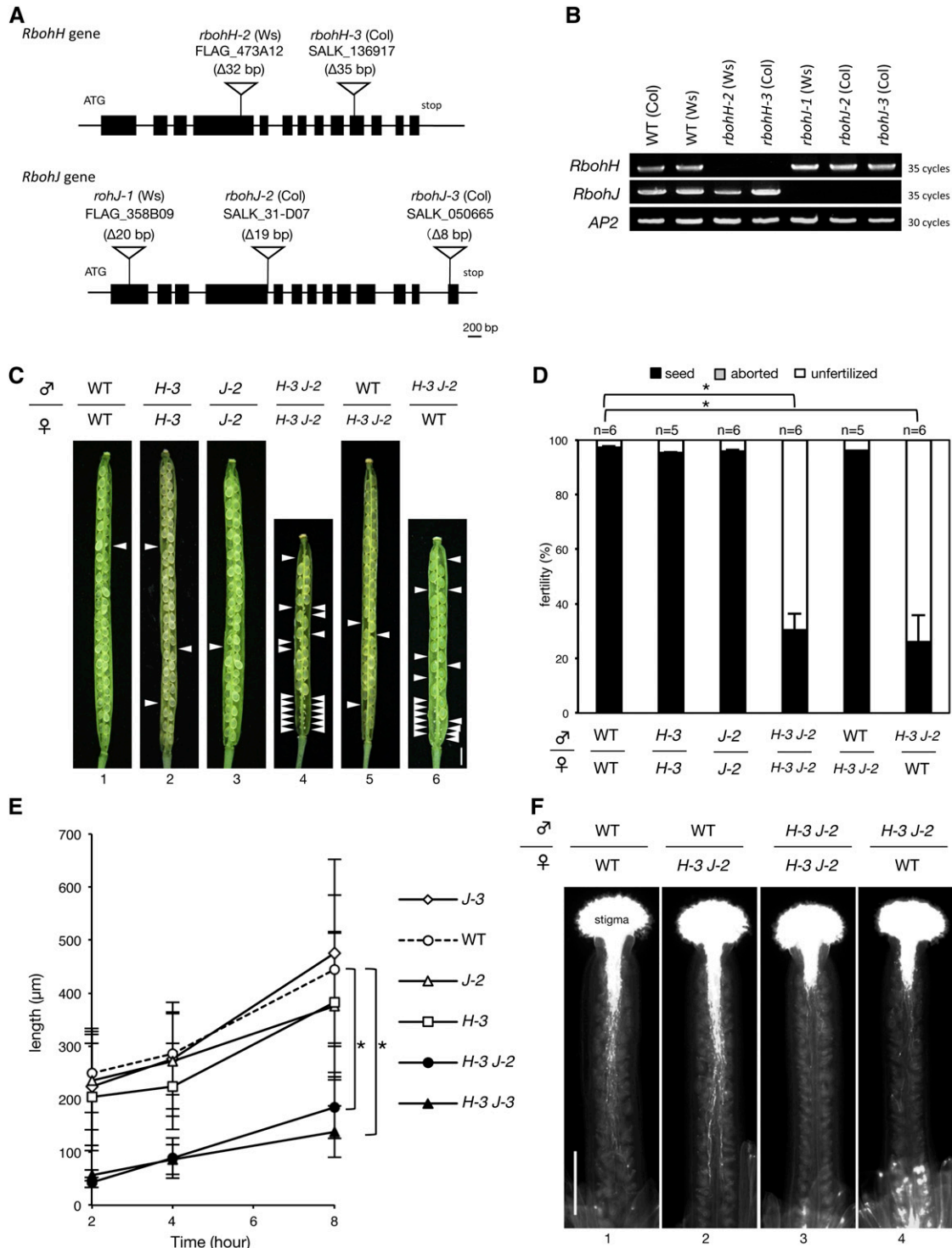
Figure 2. The *rbohH rbohJ* Double Mutant Was Defective in Pollen Tube Tip Growth.

(A) Schematic representation of the T-DNA insertions in *RbohH* and *RbohJ*. Open triangles show the sites of T-DNA insertions in the mutant together with deleted nucleotide numbers. Closed boxes indicate the protein-coding exons. *rbohH-2* and *rbohJ-1* mutants were in the Ws background, and *rbohH-3*, *rbohJ-2*, and *rbohJ-3* were in the Col-0 background.

(B) RT-PCR analysis of the full-length transcripts of *rbohH* and *RbohJ* expressed in each mutant flower. *AP2* was used as a control. Two biological and technical replicates were performed.

seeds on average (Figure 2D). A similar result was obtained using a double mutant of different alleles (*rbohH-2 rbohJ-1*) but not with the corresponding single mutants (Supplemental Figure 3). These results indicate that the fertilization defect in the *rbohH rbohJ* double mutants was attributable to the pollen grains but not to the pistils.

When germinated in vitro, the pollen tubes of each single mutant and the wild type were similar in length after 8 h, while those of the *rbohH-3 rbohJ-2* and *rbohH-3 rbohJ-3* double mutants were significantly shorter (Figure 2E). To observe the growth of pollen tubes in vivo, the pollen tubes were visualized with aniline blue staining 12 h after hand pollination. The wild-type pollen tubes extended through the style and even reached the ovules at the base of the silique regardless of the genotype of the pistil (Figure 2F, panels 1 and 2). In comparison, the *rbohH-3 rbohJ-2* pollen tubes grew through the style but barely reached the ovules, even though the pistil was wild type (Figure 2F, panels 3 and 4). These data together with those recently reported (Boisson-Dernier et al., 2013) suggest that *RbohH* and *RbohJ* are redundantly involved in pollen tube tip growth, which is required for adequate fertilization.

ROS Accumulation in the Pollen Tube Cell Wall after Pollination Is Impaired in the *rbohH rbohJ* Double Mutant

Both *RbohH* and *RbohJ* were expressed in pollen tubes (Figures 1B to 1D), suggesting that both genes may affect ROS accumulation there. To examine the ROS accumulation in pollen tubes germinated in vivo, we pollinated wild-type pistils with either wild-type or *rbohH-3 rbohJ-2* double mutant pollen grains using a micromanipulator. ROS were visualized using the fluorescent ROS indicator Oxyburst Green. Fluorescence was observed in the growing pollen tube of the wild type (Figures 3A to 3D; Supplemental Movies 1 to 3 and Supplemental Figure 4), while the fluorescence intensity in *rbohH-3 rbohJ-2* pollen tubes was much lower (Figures 3E to 3H; Supplemental Movies 4 to 6 and Supplemental Figure 4). These results in vivo are consistent with the recent report that the *rbohH rbohJ* double mutant is defective in ROS accumulation in the tip of pollen tubes germinated in vitro (Boisson-Dernier et al., 2013). This supports our idea that both *RbohH* and *RbohJ* are involved in ROS accumulation in pollen tubes in vivo.

RbohH and RbohJ Possess Ionomycin-Induced ROS-Producing NADPH Oxidase Activity

Both RbohH and RbohJ contain two EF-hand motifs in their N-terminal cytosolic regions (Figure 4A; Supplemental Figure
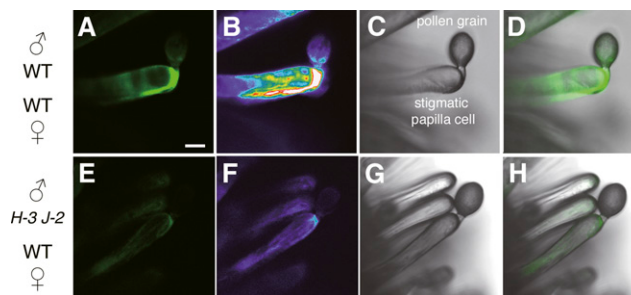

Figure 3. Detection of ROS on Stigmatic Papilla Cells.

Detection of ROS is shown on stigmatic papilla cells with Oxyburst Green 20 min after pollination.
(A) to **(D)** Intense fluorescence of Oxyburst Green around a wild-type pollen tube growing within the stigmatic papilla cell wall.
(E) to **(H)** Faint fluorescence of Oxyburst Green around the *rbohH-3 rbohJ-2* double mutant pollen tube growing within the stigmatic papilla cell wall.
(A) and **(E)** show fluorescence images; **(B)** and **(F)** show pseudocolor fluorescence images; **(C)** and **(G)** show bright-field images; and **(D)** and **(H)** show overlay images. Bar = 10 μm.

1B), suggesting that both have Ca^{2+}-activated ROS-producing activity like RbohC, RbohD, and RbohF (Ogasawara et al., 2008; Takeda et al., 2008; Kimura et al., 2012). To examine the ROS-producing activity of RbohH and RbohJ and their regulation by Ca^{2+}, each gene was transiently expressed in HEK293T cells. HEK293T cells lack Ca^{2+}-activated ROS-producing activity (Bánfi et al., 2001), allowing us to quantitatively monitor the ROS production corresponding to the exogenously expressed gene with high temporal resolution. HEK293T cells were transfected with *FLAG:RbohH-WT* and *FLAG:RbohJ-WT* (Supplemental Figure 2) and with empty vector. The expression of FLAG-tagged wild-type RbohH and RbohJ proteins in HEK293T cells was confirmed by immunoblot analysis with anti-FLAG antibody (Figures 4B and 4C). The transfected HEK293T cells were treated with ionomycin, a Ca^{2+} ionophore that induces Ca^{2+} influx into cells. Ionomycin transiently induced ROS production in *FLAG:RbohH-WT*–and *FLAG:RbohJ-WT*–transfected cells but not in empty vector–transfected cells (Figures 4B and 4C). To determine whether the ionomycin-induced ROS production of RbohH and RbohJ was attributable to NOX enzyme activity, we pretreated transfected cells with a NOX inhibitor, DPI. DPI inhibited ionomycin-induced ROS production in a dose-dependent manner (Figures 4D and 4E). These results suggest that both RbohH and RbohJ possess Ca^{2+}-activated ROS-producing NADPH oxidase activity.

Figure 2. (continued).

(C) Dissected siliques harvested ∼7 d after hand pollination. White arrowheads indicate unfertilized ovules. ♂ indicates the genotype of the pollen grain, and ♀ indicates the genotype of the pistil. Bar = 1 mm.
(D) Percentage of normal seeds, aborted seeds, and unfertilized ovules in siliques. Siliques were harvested 5 to 10 d after hand pollination. Closed bars indicate normal seeds; gray bars indicate aborted seeds; open bars indicate unfertilized ovules. Values are means ± SE (*n* = 5 to 6 siliques); *P < 0.01 (Student's *t* test).
(E) Length of pollen tubes germinated in vitro. Values are means ± SD (*n* = 11–30); *P < 0.01 (Student's *t* test).
(F) Pollen tubes were visualized by aniline blue staining in vivo. Pistils were harvested 12 h after hand pollination. Bar = 500 μm.

Figure 4. Ca²⁺ Activates the ROS-Producing Activity of RbohH and RbohJ via the EF-Hand Motif.

(A) Amino acid sequences of wild-type and mutant EF-hand regions of RbohH and RbohJ. Two EF-hand motifs are indicated. The Ca^{2+} binding loops in the first and second EF-hand motifs are boxed. The consensus Ca^{2+} binding loop is shown: X, Y, Z, #, and –X = Ca^{2+} ligand; –Z = Ca^{2+} ligand, a bidentate Glu (E) or Asp (D); G = Gly; I = Ile or other aliphatic residue found at this position; * = any residue.
(B) and **(C)** Ionomycin-induced ROS production of RbohH **(B)** and RbohJ **(C)** in HEK293T cells. FLAG-tagged proteins of the wild type and EF-hand mutants were transiently expressed in HEK293T cells. After 5 min of baseline measurement, 1 μM ionomycin was added to the medium. Expressed proteins were detected by immunoblotting with anti-FLAG antibody. As a loading control, β-actin was used.
(D) and **(E)** Dose-dependent inhibition of ionomycin-induced ROS production by DPI. HEK293T cells transiently expressing FLAG-tagged RbohH **(D)** or RbohJ **(E)** were pretreated with different concentrations of DPI. After 5 min of baseline measurement, 1 μM ionomycin was added to the medium.
For **(B)** to **(E)**, all quantified data are means ± se (n = 3). Arrows indicate the time at which ionomycin was added. ROS production was measured by chemiluminescence and expressed as relative luminescence units per second (RLU/s). The maximum value of the luminescence activity was set at 1.0 unit.

The canonical EF-hand motif has a Ca^{2+} binding loop consisting of 12 amino acid residues. The amino acids at the X and $-Z$ positions of the Ca^{2+} binding loop are critical for Ca^{2+} chelation (Figure 4A) (Grabarek, 2006; Gifford et al., 2007). To determine the role of the two EF-hand motifs in the ionomycin-induced ROS-producing activity of RbohH and RbohJ, we introduced point mutations into the first (RbohH-D208A, RbohJ-D218A, RbohH-E219Q, and RbohJ-E229Q; X and $-Z$ positions) and second (RbohH-D252A and RbohJ-D262A; X position) EF-hand motifs (Figure 4A). Immunoblot analysis showed that the amino acid substitutions did not affect the expression levels of RbohH and RbohJ (Figures 4B and 4C). However, ionomycin-induced ROS production by both proteins was severely reduced by both pairs of mutations (Figures 4B and 4C). The EF-hand motifs of *Arabidopsis* RbohD, *Arabidopsis* RbohF (formerly RbohA), and rice (*Oryza sativa*) RbohB bind Ca^{2+}, and their EF-hand mutations impaired Ca^{2+}-induced ROS-producing activity (Keller et al., 1998; Ogasawara et al., 2008; Oda et al., 2010; Kimura et al., 2012; Takahashi et al., 2012). These results suggest that Ca^{2+}-dependent activation mediated by the EF-hand motif is conserved among plant Rboh proteins, including RbohH and RbohJ.

Interestingly, the amino acid in the $-Z$ position of the second EF-hand motif of RbohH and RbohJ is Gln (Q), which differs from the conserved residue (Glu [E] or Asp [D]). This implies that the Ca^{2+}-activated ROS-producing activity of RbohH and RbohJ may not be fully functional. If so, the *RbohH-Q263E* and *RbohJ-Q273E* mutations may increase the Ca^{2+} affinity of the second EF-hand motif and increase their activities. However, unexpectedly, these mutants showed decreased ionomycin-induced ROS-producing activity (Figures 4B and 4C). This result is consistent with our previous data that a nonbidentate residue (Gln or Asn) at the $-Z$ position of the Ca^{2+} binding loop in the second EF-hand motif of RbohD has an important role in Ca^{2+}-induced conformational change in the EF-hand rather than Ca^{2+} binding (Ogasawara et al., 2008), suggesting that RbohH and RbohJ require a conformational change in the second EF-hand region for the Ca^{2+}-dependent activation of ROS-producing activity, as does RbohD.

RbohH and RbohJ Are Synergistically Activated by Calyculin A and Ionomycin

Arabidopsis RbohC/RHD2, RbohD, and RbohF and rice RbohB are activated not only by Ca^{2+} but also by protein phosphorylation (Ogasawara et al., 2008; Takeda et al., 2008; Kimura et al., 2012; Takahashi et al., 2012). To test whether the ROS-producing activity of *Arabidopsis* RbohH and RbohJ are also activated by protein phosphorylation, *FLAG:RbohH-* and *FLAG:RbohJ-* transfected HEK293T cells were treated with calyculin A, a Ser/Thr protein phosphatase inhibitor. Calyculin A enhances the protein phosphorylation of RbohD and induces ROS production in *RbohD*-transfected HEK293T cells (Ogasawara et al., 2008). Calyculin A induced ROS production in *FLAG:RbohH-* or *FLAG:RbohJ*-transfected cells but not in empty vector–transfected cells, suggesting that the ROS-producing activity of RbohH and RbohJ is activated by protein phosphorylation (Figures 5A and 5B, insets). Calyculin A–induced ROS production was much lower than ionomycin-induced ROS production in both transfected cells; however, pretreatment with calyculin A enhanced the ionomycin-

induced ROS-producing activity: the ROS-producing activity of RbohH and RbohJ in the cells treated with both calyculin A and ionomycin was nine times and five times higher than that in cells treated with ionomycin alone, respectively (Figures 5A and 5B). These results suggest that RbohH and RbohJ are synergistically activated by protein phosphorylation and Ca^{2+}.

RbohH and RbohJ Are Localized at the Plasma Membrane of the Growing Tips of Pollen Tubes

To examine the localization of RbohH and RbohJ in pollen tubes, we generated transgenic plants expressing GFP-tagged wild-type RbohH (*GFP:RbohH-WT*) and wild-type RbohJ (*GFP:*
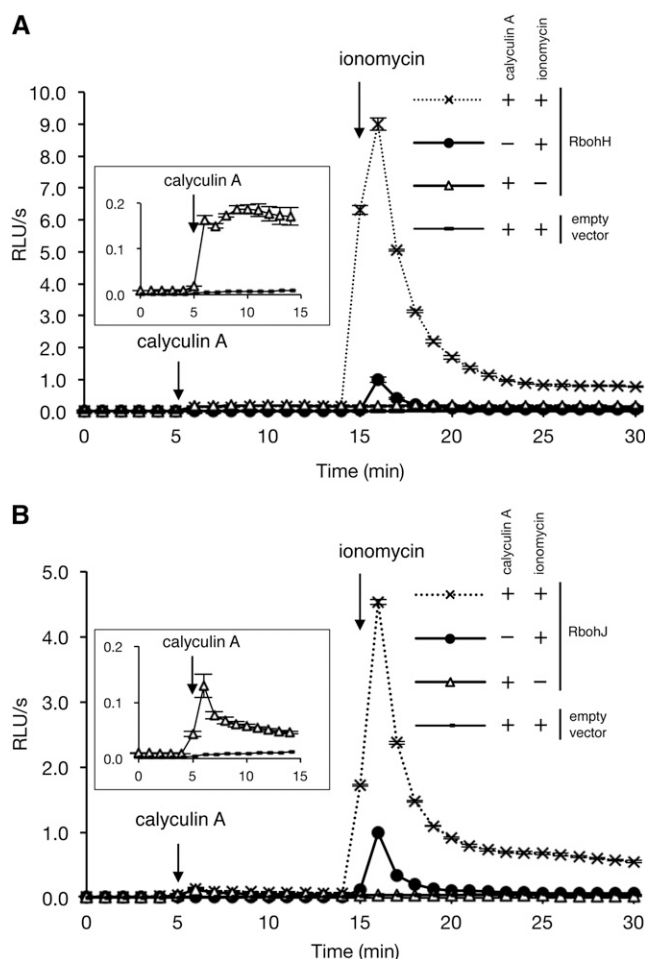
Figure 5. Synergistic Activation of RbohH and RbohJ by Calyculin A and Ionomycin.

HEK293T cells were transiently transfected with FLAG-tagged *RbohH* **(A)** or *RbohJ* **(B)**. After baseline measurement, either or both 0.1 µM calyculin A or 1 µM ionomycin was added to the medium at the time points indicated by the arrows. Insets show enlarged diagrams of calyculin A–induced ROS production for 15 min. All quantified data are means ± SE (*n* = 3). ROS production was measured by chemiluminescence and expressed as relative luminescence units per second (RLU/s). The maximum value of ionomycin-induced luminescence activity was set at 1.0 unit.
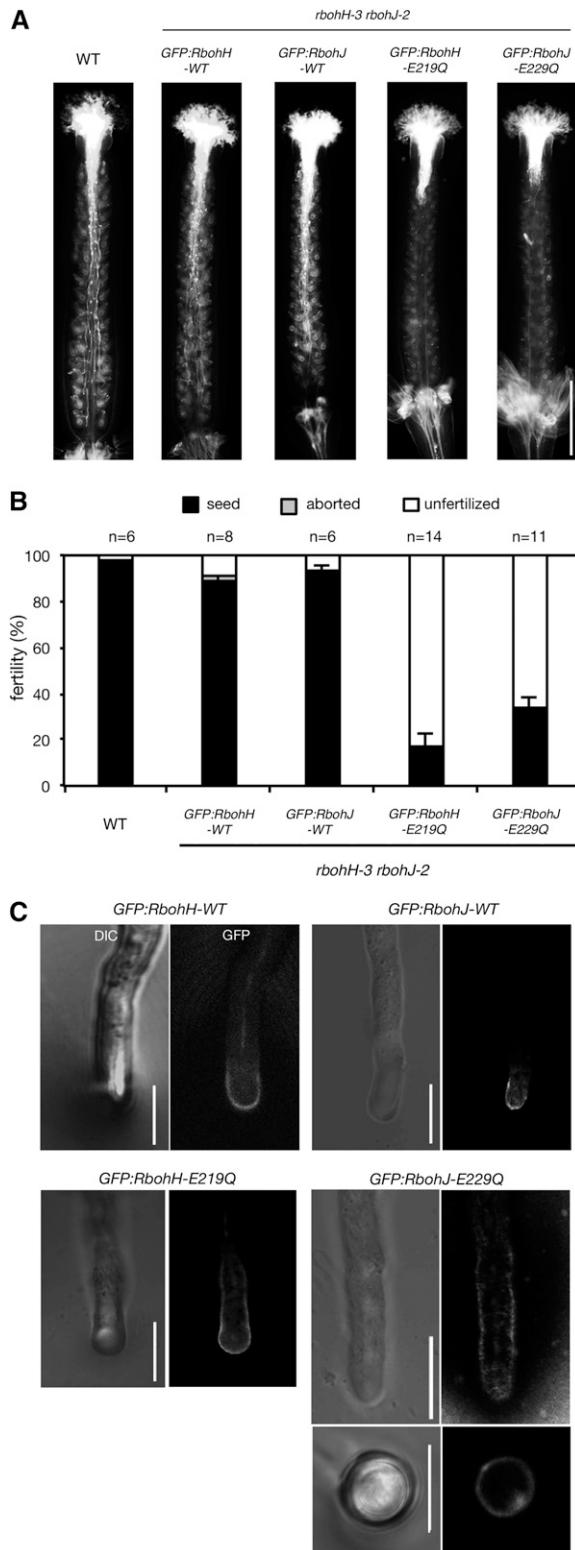
Figure 6. EF-Hand Mutations Affect Pollen Tube Tip Growth but Not Protein Subcellular Localization.

(A) and **(B)** Complementation analysis of the *rbohH-3 rbohJ-2* double mutant phenotype with GFP-tagged wild-type or EF-hand mutants

RbohJ-WT) under the control of their respective native promoters in the *rbohH-3 rbohJ-2* double mutant background (Supplemental Figure 2). To test whether the GFP-tagged RbohH and RbohJ proteins are functional, wild-type pistils were pollinated with the pollen grains of homozygous transgenic *rbohH-3 rbohJ-2* plants expressing *GFP:RbohH-WT* or *GFP:RbohJ-WT*, and pollen tubes were visualized in vivo by aniline blue staining (Figure 6A). The elongation of these pollen tubes was comparable to that of the wild type (Figure 6A). The expression of *GFP:RbohH-WT* or *GFP:RbohJ-WT* also rescued the fertility defect in the *rbohH-3 rbohJ-2* double mutant (Figure 6B). These results indicate that GFP-tagged RbohH and RbohJ proteins are functional in pollen tube growth.

GFP fluorescence in the transgenic *rbohH-3 rbohJ-2* double mutant plants expressing *GFP:RbohH-WT* and *GFP:RbohJ-WT* by the respective native promoter and terminator was analyzed by confocal microscopy. GFP fluorescence was observed at the plasma membrane periphery of the pollen tube tip (Figure 6C). These results are consistent with the recent report that GFP-tagged RbohH protein, overexpressed under the control of the 35S promoter, is localized in the plasma membrane of the pollen tube tip (Boisson-Dernier et al., 2013) and also with the plasma membrane localization of RbohC/RHD2 and RbohF (Keller et al., 1998; Takeda et al., 2008; Kawarazaki et al., 2013; Kimura et al., 2013), suggesting that both RbohH and RbohJ function at the plasma membrane of the growing pollen tube tip.

EF-Hand Motifs of RbohH and RbohJ Are Necessary for Proper Pollen Tube Tip Growth

The point mutations in the EF-hand motifs reduced the ionomycin-induced ROS-producing activities of RbohH and RbohJ (Figures 4B and 4C). To examine whether the EF-hand motifs of RbohH and RbohJ functioned in pollen tube tip growth, we generated transgenic plants to express GFP-tagged EF-hand mutants of the proteins under the control of their respective native promoters in

---

(E219Q and E229Q). Pollen grains were from wild-type or homozygous transgenic plants. *GFP:RbohH-WT* and *GFP:RbohH-E219Q* were expressed under the control of the *RbohH* promoter in the *rbohH-3 rbohJ-2* double mutant, while *GFP:RbohJ-WT* and *GFP:RbohJ-E229Q* were expressed under the control of the *RbohJ* promoter in the *rbohH-2 rbohJ-2* double mutant. Pistils were wild type (Col-0).

(A) Pistils were harvested 12 h after hand pollination and stained with aniline blue. Bar = 500 μm.

(B) Percentage of normal seeds, aborted seeds, and unfertilized ovules in siliques. Siliques were harvested 5 to 10 d after hand pollination. Closed bars indicate normal seeds; gray bars indicate aborted seeds; open bars indicate unfertilized ovules. Values are means ± SE (*n* = 6 to 11 siliques).

(C) Subcellular localization of GFP-tagged wild-type and EF-hand mutants (E219Q and E229Q) in pollen tubes of the *rbohH-3 rbohJ-2* double mutant. Pollen grains were germinated in vitro. *GFP:RbohH-WT* and *GFP:RbohH-E219Q* were expressed under the control of the *RbohH* promoter in the *rbohH-3 rbohJ-2* double mutant, while *GFP:RbohJ-WT* and *GFP:RbohJ-E229Q* were expressed under the control of the *RbohJ* promoter in the *rbohH-3 rbohJ-2* double mutant. The bottom right panel shows a cross section of a pollen tube expressing *GFP:RbohJ-E229Q*. Bars = 10 μm.

the *rbohH-3 rbohJ-2* double mutant background. GFP fluorescence in both mutants was observed at the plasma membrane periphery of the pollen tube, similar to that in the wild type (Figure 6C). GFP fluorescence in the *GFP:RbohJ-E229Q* mutant was observed at the cell periphery in the transverse section of the pollen tube (Figure 6C, bottom right side). These observations indicate that the mutations in the EF-hand motifs did not significantly affect the subcellular localization of RbohH and RbohJ in the pollen tube. We examined pollen tube length in vivo and the fertility of wild-type and homozygous transgenic plants expressing the EF-hand mutant. Neither the expression of *GFP:RbohH-E219Q* nor *GFP:RbohJ-E229Q* could complement the *rbohH-3 rbohJ-2* double mutant phenotype (Figures 6A and 6B). These results suggest that the EF-hand motifs of RbohH and RbohJ are critical to pollen tube tip growth due to their regulation of ROS-producing activity.

DISCUSSION

Pollen tube tip growth is a central process in plant fertilization. Here, we showed that two NOX proteins, RbohH and RbohJ, are involved in pollen tube tip growth in *Arabidopsis*. The *rbohH rbohJ* double mutant was defective in pollen tube tip growth and accumulated fewer ROS in the growing pollen tubes compared with the wild type. RbohH and RbohJ also showed ionomycin-induced ROS-producing activities that were impaired by EF-hand mutations. Both GFP-tagged RbohH and RbohJ were localized at the plasma membrane of the pollen tube. These results suggest that Ca^{2+}-activated ROS production by RbohH and RbohJ is essential for proper pollen tube tip growth and contributes to subsequent fertilization. Meanwhile, NADPH oxidase in pollen has been proposed to produce ROS in lung epithelium, causing oxidative stress and augmenting allergic airway inflammation induced by pollen antigens (Boldogh et al., 2005). Our identification here of the molecules involved in enzymatic ROS production in pollen may also be relevant to allergen research.

RbohH and RbohJ Are Primary Sources of ROS in Growing Pollen Tubes

A NOX inhibitor, DPI, significantly inhibits growth and ROS accumulation in pollen tubes (Potocký et al., 2007). In the *rbohH-3 rbohJ-2* double mutant, ROS accumulation in growing pollen tubes was impaired in vivo and in vitro (Figure 3; Boisson-Dernier et al., 2013). Both RbohH and RbohJ showed ROS-producing activity that was inhibited by DPI (Figure 4). These data suggest that RbohH and RbohJ are the major ROS-producing enzymes in pollen tubes.

In contrast, the elongation of pollen tubes in the *rbohH rbohJ* double mutant was not completely inhibited (Figure 2F). A recent Ca^{2+} imaging study showed that disruption of *RbohH* and *RbohJ* affects but does not abolish the tip-focused Ca^{2+} gradient (Boisson-Dernier et al., 2013). These findings imply that another *Rboh* gene may also function in pollen tube growth. According to the *Arabidopsis* eFP Browser microarray database (Schmid et al., 2005; Winter et al., 2007), *RbohA*, *RbohE*, and *RbohI* are expressed in pollen, although their expression levels are one-fiftieth or less than that of *RbohH*. Their functions in plant cells and enzyme activities have not yet been reported. One or more may

also play a role in pollen tube tip growth through ROS production. Alternatively, other kinds of ROS-producing enzymes, such as class III cell wall peroxidases and/or polyamine oxidases (Wu et al., 2010; O'Brien et al., 2012), may also be involved in pollen tube tip growth.

Regulation of Activity and Subcellular Localization of RbohH and RbohJ at the Tip of Pollen Tubes

A Rho-type GTPase, ROP1, one of 11 ROPs in *Arabidopsis*, is localized in the pollen tube and functions as a major regulator of tip growth (Lin et al., 1996; Li et al., 1999; Qin and Yang, 2011). Rice Rac1, a ROP ortholog, binds the N-terminal region of Os-RbohB to regulate defense responses (Wong et al., 2007). Because RbohH and RbohJ were localized to the pollen tube tip (Figure 6C), the *Arabidopsis* ROP1 may bind to the N-terminal region of RbohH and RbohJ and regulate their activity.

Alternatively, ROP1 may be involved in targeting RbohH and RbohJ to the tips of pollen tubes. ROP1 activates two counteracting pathways: (1) Ca^{2+} signaling leading to F-actin disassembly by binding to RIC3 (for ROP-interactive CRIB-containing protein 3), and (2) promoting F-actin assembly by binding to RIC4 (Gu et al., 2005). In root hairs, RhoGDI, a regulator of ROP GTPase, regulates the spatial distribution of ROP2 and the sites of ROS production at the growing tip (Carol et al., 2005). Moreover, the overexpression of ROP2 in root hairs caused ectopic accumulation of ROS and deformation of the hair cells in the wild type but not in a mutant of RbohC/RHD2 (Jones et al., 2007). These findings suggest that the ROP GTPase can regulate the spatial localization of Rboh proteins and thus the site of ROS production in polarized cells. Therefore, it is possible that ROP1 regulates pollen tube tip growth by confining the subcellular localization of RbohH and RbohJ to the growing tip. A future goal is to investigate the functional relationships between ROP1 and these Rboh proteins to understand how directional growth is activated and spatially regulated during pollen tube tip growth.

The activity and subcellular localization of some plant Rbohs have also been shown to be regulated by phosphorylation by several families of protein kinases, including calcium-dependent protein kinases, SnRKs, and CIPKs (Sirichandra et al., 2009; Asai et al., 2013; Drerup et al., 2013; Dubiella et al., 2013; Kimura et al., 2013). The present data suggest that both RbohH and RbohJ are also activated by protein phosphorylation, and both protein phosphorylation and Ca^{2+} show a synergistic effect on the activation of RbohH and RbohJ (Figure 5). Together with the results on RbohC/RHD2, RbohD, and RbohF as well as Os-RbohB (Ogasawara et al., 2008; Takeda et al., 2008; Kimura et al., 2012; Takahashi et al., 2012), the synergistic activation may be a general regulatory mechanism for the ROS-producing activity of Rboh proteins. *ANXUR1* overexpression phenotypes are dependent on the functions of *RbohH* and *RbohJ*, suggesting that RbohH and RbohJ are positive downstream effectors in the ANXUR receptor-like kinase–dependent pathway in *Arabidopsis* (Boisson-Dernier et al., 2013). FERONIA, a homolog of ANXUR (Boisson-Dernier et al., 2009; Miyazaki et al., 2009), binds a peptide hormone, rapid alkalinization factor (RALF), to regulate cell expansion (Haruta et al., 2014). Some RALF-like peptides are expressed in pollen (Haruta et al., 2014). These results imply the existence of a novel mechanism for the ROS-mediated regulation of pollen tube tip

growth; ANXUR receptor-like kinase may be activated by RALF-like peptides to play a role in the phosphorylation-dependent activation of RbohH and RbohJ directly or indirectly.

Possible Positive Feedback Regulation of Pollen Tube Tip Growth Mediated by Ca^{2+} and ROS

In root hair cells of *Arabidopsis*, the ROS produced by RbohC/RHD2 has been suggested to activate Ca^{2+}-permeable channel(s) that transport Ca^{2+} into the cells, where it in turn activates RbohC/RHD2 via its EF-hand motifs. This positive feedback provides a mechanism to explain how cells such as root hairs maintain polarity during morphogenesis (Foreman et al., 2003; Takeda et al., 2008). Many similarities in the molecular mechanisms of tip growth in root hairs and pollen tubes have been discussed (Gu and Nielsen, 2013), suggesting that a similar positive feedback mechanism may be involved in pollen tube tip growth. The EF-hand mutants of RbohH and RbohJ showed impaired ionomycin-induced ROS-producing activity and inhibited pollen tube tip growth in vivo, although their subcellular localizations were not affected (Figures 4 and 5), suggesting that the ROS production mediated by RbohH and RbohJ in the growing pollen tubes depends on Ca^{2+}. Application of external Ca^{2+} induced ROS accumulation at the tips of both pollen tubes and root hairs (Foreman et al., 2003; Potocký et al., 2007, 2012). In turn, ROS-activated plasma membrane Ca^{2+}-permeable channels have been detected in pollen tubes and were suggested to mediate Ca^{2+} influx into the cells (Wu et al., 2010). Because the regulation of ROS production in pollen tubes by RbohH and RbohJ shown in the present study resembled the situation in root hairs, we propose that a similar positive feedback mechanism at the apex of pollen tubes plays a key role in polarized cell growth. NOX, ROS, and GTPase are also involved in fungal hyphal morphogenesis (Coelho et al., 2008; Takemoto et al., 2011), implying that the positive feedback regulation in localized cell growth may be broadly conserved during evolution in many eukaryotic cells, including plants and fungi.

ROS Produced by RbohH and RbohJ May Contribute to Cell Wall Structure

RbohH and *RbohJ* play a role in ROS production in growing pollen tubes in vitro (Boisson-Dernier et al., 2013) and in vivo (Figure 3). Apoplastic ROS production at the apex of pollen tubes may also be involved in cell growth. ROS, including hydroxyl radicals, have been suggested to be involved in cell elongation by loosening the cell wall in maize (*Zea mays*) coleoptiles, leaves, and roots (Schopfer, 2001; Rodríguez et al., 2002; Liszkay et al., 2004). This cell wall loosening may be achieved by the "oxidative scission" of cell wall polysaccharides by hydroxyl radicals (Fry, 1998). The apoplastic production of superoxide anion radicals can be associated with the generation of hydroxyl radicals by the Fenton reaction (Kuchitsu et al., 1995). Because tip-growing cells such as pollen tubes and root hairs grow much faster than do other types of cells, Rboh-mediated ROS production may function in maintaining the flexibility of newly formed cell walls at the tip. In contrast, NOX-mediated ROS production has also been suggested to be involved in cross-linking various cell wall components by providing the substrate hydrogen peroxide for apoplastic peroxidases (O'Brien et al., 2012). The pollen tubes of the *rbohH rbohJ*

double mutant rupture easily in vitro (Boisson-Dernier et al., 2013). Therefore, some molecular species of ROS may function in cross-linking while others may act in cell wall loosening to shape the long cylindrical pollen tubes. Our findings on the molecular mechanisms and regulation of deliberate ROS production in the pollen tubes will contribute to further dissection of the physiological significance of apoplastic ROS production in polarized cell elongation.

METHODS

Plant Material

The T-DNA insertion mutants of *rbohH-2* (FLAG_473A12) and *rbohJ-1* (FLAG_358B09) from *Arabidopsis thaliana* background Wassilewskija (Ws) and *rbohH-3* (SALK_136917), *rbohJ-2* (SAIL-31-D07), and *rbohJ-3* (SALK_050665) from Col-0 were used. All mutants were backcrossed to their parent genetic background (Ws or Col-0) more than three times.

Plasmid Constructs

The coding DNA sequence (CDS) of *RbohH* and *RbohJ* genes was amplified by PCR from a cDNA library of *Arabidopsis*. *RbohH$_{pro}$:GUS* and *RbohJ$_{pro}$: GUS* constructs were generated by cloning the promoter and terminator regions of *RbohH* and *RbohJ* into the pBIN19 binary vector with the CDS region of GUS for expression in the *Arabidopsis* Col-0 wild type (Supplemental Figure 2). *RbohH$_{pro}$:GFP:RbohH* and *RbohJ$_{pro}$:GFP:RbohJ* constructs were generated by cloning the promoter, terminator, and CDS regions of *RbohH* and *RbohJ* into the pZP2H-lac binary vector with a CDS region of *Aequorea coerulescens GFP1* (Takara) to express the GFP-fused RbohH and RbohJ in the *rbohH-2 rbohJ-2* double mutant (Supplemental Figure 2). *RbohH$_{pro}$:RbohH* and *RbohJ$_{pro}$:RbohJ* constructs were generated by cloning the promoter and terminator regions of *RbohH* and *RbohJ* and the CDS region of *RbohH* and *RbohJ* into the pBIN19 binary vector for expression in the *rbohH-3 rbohJ-2* double mutant (Supplemental Figure 2). *FLAG:RbohH* and *FLAG:RbohJ* constructs were generated by introducing the CDS region of *RbohH* and *RbohJ* into the pcDNA3.1(–) vector (Life Technologies) with the 3×FLAG sequence (Sigma-Aldrich) at their 5′ ends for expression in HEK293T cells. The codon-optimized synthetic CDS of *RbohJ* was used for expression in HEK293T cells. The EF-hand mutants of *RbohH* and *RbohJ* were generated by PCR with mutant primers.

Histochemical Staining of GUS Activity

Flowers were fixed in 90% acetone at –20°C for 1 h. The fixed flowers were then briefly washed twice with 100 mM NaPO$_4$, pH 7.4, and placed into GUS reaction solution (0.5 mg/mL 5-bromo-4-chloro-3-indolyl-β-D-glucuronide, 0.5 mM potassium ferricyanide/ferrocyanide, and 100 mM NaPO$_4$, pH 7.4) for 18 to 48 h at 37°C. The stained flowers were cleared in a 50 to 99.5% ethanol series and then hydrated before observations were made.

Fertility

Flowers were emasculated 1 d before the crossing experiment. Five to 10 d after hand pollination, siliques were dissected and observed with a microscope. Seeds in the siliques were counted to analyze the fertility in each cross.

Aniline Blue Staining

Pistils were collected 12 h after hand pollination and fixed overnight in acetic acid:ethanol solution (25:75) at room temperature. The fixed pistils were softened in 1 N NaOH for 30 min at 60°C and then stained with 0.01% aniline blue in 2% potassium phosphate buffer (K$_3$PO$_4$) for several

hours in the dark. Fluorescence images were taken with a fluorescence microscope.

Measurement of Pollen Tube Lengths

To measure the lengths of the pollen tubes, pollen grains were germinated in vitro on pollen tube germination medium (Boavida and McCormick, 2007). A thin layer of the germination medium containing 1% NuSieve GTG Agarose (Lonza) was placed on a cover slip, and pollen grains were germinated on it. After 2, 4, and 8 h, images were captured with a Hamamatsu charge-coupled device camera and processed with Photoshop CS5 software (Adobe Systems), and pollen tubes were measured using ImageJ (National Institutes of Health) software.

Oxyburst Green Assay

The flowers of wild-type (Col-0) *Arabidopsis* whose anthers were removed before dehiscence were excised and attached to an agar plate. A drop of 20 μM Oxyburst Green (Life Technologies) solution containing 0.005% Tween 20 was put on the stigma and air-dried for 1 h. The pistil was mounted on a cover slip, and a pollen grain from a freshly dehisced anther of the wild type or *rbohH-3 rbohJ-2* was placed on it using a micromanipulator. The pistil was observed by confocal microscopy (LSM710; Zeiss), excited with 488 nm using a Plan-Apo 20×/0.8 objective lens. Fluorescence emission from 500 to 530 nm was captured.

Cell Culture and Transfection

HEK293T cells were maintained at 37°C in 5% CO_2 in Dulbecco's Modified Eagle's Medium nutrient mixture Ham's F-12 (WAKO) supplemented with 10% fetal bovine serum (HyClone). HEK293T cells were transiently transfected with the vector plasmids for gene expression using the GeneJuice transfection regent (Novagen) according to the manufacturer's protocol.

Measurement of ROS Production in HEK293T Cells

The ROS-producing activity of plant Rboh was determined as described previously (Ogasawara et al., 2008; Takeda et al., 2008; Kimura et al., 2012; Takahashi et al., 2012; Kawarazaki et al., 2013; Kimura et al., 2013). ROS production was detected by a luminol-amplified chemiluminescence technique. Chemiluminescence was measured every 1 min at 37°C using a microplate luminometer (Centro LB960; Berthold Technologies). ROS production was expressed in relative luminescence units per second. Data are averages of three samples in a representative experiment. We independently replicated this experiment more than 10 times with similar results.

Immunoblot Analysis

The cell lysates from transfected HEK293T cells were separated by 7.5% SDS-PAGE and transferred to a polyvinylidene difluoride membrane (Immobilon P; Millipore). The following antibodies were diluted in Can Get Signal Immunoreaction Enhancer Solution (NKB-101T; Toyobo): anti-FLAG M2 (F1804; Sigma-Aldrich), 1:3000; anti-β-actin (A5316; Sigma-Aldrich), 1:5000; and anti-mouse IgG (NA931; GE Healthcare), 1:5000.

GFP Imaging

For GFP imaging, pollen tubes were grown in vitro. GFP fluorescence was excited with a 488-nm argon laser. Images were captured using a Zeiss LSM510 or LSM700 inverted confocal microscope and processed with Adobe Photoshop CS5 software.

Accession Numbers

Sequence data from this article can be found in the Arabidopsis Genome Initiative or GenBank/EMBL databases under the following accession numbers: *RbohH* (At5g60010) and *RbohJ* (At3g45810).

Supplemental Data

The following materials are available in the online version of this article.

Supplemental Figure 1. Phylogenetic Tree of *Arabidopsis* Rboh and the Domain Structure of Rboh.

Supplemental Figure 2. Plasmid Construction.

Supplemental Figure 3. The *rbohH-2 rbohJ-1* Double Mutant (Ws Background) Had Reduced Fertility.

Supplemental Figure 4. Still Images of Supplemental Movies 1 to 6.

Supplemental Table 1. Sequences of the Primers Used in This Work.

Supplemental Movie 1. Detection of ROS on a Wild-Type Stigmatic Papilla Cell after Pollination with a Wild-Type Pollen Grain, Fluorescence Images.

Supplemental Movie 2. Detection of ROS on a Wild-Type Stigmatic Papilla Cell after Pollination with a Wild-Type Pollen Grain, Bright-Field Images.

Supplemental Movie 3. Detection of ROS on a Wild-Type Stigmatic Papilla Cell after Pollination with a Wild-Type Pollen Grain, Overlay Images.

Supplemental Movie 4. Detection of ROS on a Wild-Type Stigmatic Papilla Cell after Pollination with an *rbohH-3 rbohJ-2* Double Mutant Pollen Grain, Fluorescence Images.

Supplemental Movie 5. Detection of ROS on a Wild-Type Stigmatic Papilla Cell after Pollination with an *rbohH-3 rbohJ-2* Double Mutant Grain, Bright-Field Images.

Supplemental Movie 6. Detection of ROS on a Wild-Type Stigmatic Papilla Cell after Pollination with an *rbohH-3 rbohJ-2* Double Mutant Grain, Overlay Images.

Supplemental Data Set 1. Alignments Used to Generate the Phylogeny Presented in Supplemental Figure 1A.

AUTHOR CONTRIBUTIONS

H.K. conceived and designed the experiments with the support of K.K. H.K., R.N., M.I., M.M.K., S.K., T.K., E.S., and Y.H. performed the experiments. H.K., M.I., M.M.K., S. Takeda, M.A., and K.K. wrote the article. S.K., T.H., and S. Takayama helped writing the article. H.K. and K.K. are co-corresponding authors for the article.

REFERENCES

Asai, S., Ichikawa, T., Nomura, H., Kobayashi, M., Kamiyoshihara, Y., Mori, H., Kadota, Y., Zipfel, C., Jones, J.D., and Yoshioka, H. (2013). The variable domain of a plant calcium-dependent protein kinase (CDPK) confers subcellular localization and substrate recognition for NADPH oxidase. J. Biol. Chem. **288:** 14332–14340.

Bánfi, B., Molnár, G., Maturana, A., Steger, K., Hegedûs, B., Demaurex, N., and Krause, K.H. (2001). A Ca^{2+}-activated NADPH oxidase in testis, spleen, and lymph nodes. J. Biol. Chem. **276:** 37594–37601.

Boavida, L.C., and McCormick, S. (2007). Temperature as a determinant factor for increased and reproducible in vitro pollen germination in *Arabidopsis thaliana*. Plant J. **52:** 570–582.

Boisson-Dernier, A., Lituiev, D.S., Nestorova, A., Franck, C.M., Thirugnanarajah, S., and Grossniklaus, U. (2013). ANXUR receptor-like kinases coordinate cell wall integrity with growth at the pollen tube tip via NADPH oxidases. PLoS Biol. **11:** e1001719.

Boisson-Dernier, A., Roy, S., Kritsas, K., Grobei, M.A., Jaciubek, M., Schroeder, J.I., and Grossniklaus, U. (2009). Disruption of the pollen-expressed FERONIA homologs ANXUR1 and ANXUR2 triggers pollen tube discharge. Development **136:** 3279–3288.

Boldogh, I., Bacsi, A., Choudhury, B.K., Dharajiya, N., Alam, R., Hazra, T.K., Mitra, S., Goldblum, R.M., and Sur, S. (2005). ROS generated by pollen NADPH oxidase provide a signal that augments antigen-induced allergic airway inflammation. J. Clin. Invest. **115:** 2169–2179.

Brown, D.I., and Griendling, K.K. (2009). Nox proteins in signal transduction. Free Radic. Biol. Med. **47:** 1239–1253.

Cárdenas, L., Lovy-Wheeler, A., Kunkel, J.G., and Hepler, P.K. (2008). Pollen tube growth oscillations and intracellular calcium levels are reversibly modulated by actin polymerization. Plant Physiol. **146:** 1611–1621.

Carol, R.J., Takeda, S., Linstead, P., Durrant, M.C., Kakesova, H., Derbyshire, P., Drea, S., Zarsky, V., and Dolan, L. (2005). A RhoGDP dissociation inhibitor spatially regulates growth in root hair cells. Nature **438:** 1013–1016.

Coelho, S.M., Brownlee, C., and Bothwell, J.H. (2008). A tip-high, Ca^{2+}-interdependent, reactive oxygen species gradient is associated with polarized growth in *Fucus serratus* zygotes. Planta **227:** 1037–1046.

Drerup, M.M., Schlücking, K., Hashimoto, K., Manishankar, P., Steinhorst, L., Kuchitsu, K., and Kudla, J. (2013). The calcineurin B-like calcium sensors CBL1 and CBL9 together with their interacting protein kinase CIPK26 regulate the Arabidopsis NADPH oxidase RBOHF. Mol. Plant **6:** 559–569.

Dubiella, U., Seybold, H., Durian, G., Komander, E., Lassig, R., Witte, C.P., Schulze, W.X., and Romeis, T. (2013). Calcium-dependent protein kinase/NADPH oxidase activation circuit is required for rapid defense signal propagation. Proc. Natl. Acad. Sci. USA **110:** 8744–8749.

Dutta, R., and Robinson, K.R. (2004). Identification and characterization of stretch-activated ion channels in pollen protoplasts. Plant Physiol. **135:** 1398–1406.

Feijó, J.A., Sainhas, J., Holdaway-Clarke, T., Cordeiro, M.S., Kunkel, J.G., and Hepler, P.K. (2001). Cellular oscillations and the regulation of growth: The pollen tube paradigm. Bioessays **23:** 86–94.

Foreman, J., Demidchik, V., Bothwell, J.H., Mylona, P., Miedema, H., Torres, M.A., Linstead, P., Costa, S., Brownlee, C., Jones, J.D., Davies, J.M., and Dolan, L. (2003). Reactive oxygen species produced by NADPH oxidase regulate plant cell growth. Nature **422:** 442–446.

Frietsch, S., Wang, Y.F., Sladek, C., Poulsen, L.R., Romanowsky, S.M., Schroeder, J.I., and Harper, J.F. (2007). A cyclic nucleotide-gated channel is essential for polarized tip growth of pollen. Proc. Natl. Acad. Sci. USA **104:** 14531–14536.

Fry, S.C. (1998). Oxidative scission of plant cell wall polysaccharides by ascorbate-induced hydroxyl radicals. Biochem. J. **332:** 507–515.

Gifford, J.L., Walsh, M.P., and Vogel, H.J. (2007). Structures and metal-ion-binding properties of the Ca^{2+}-binding helix-loop-helix EF-hand motifs. Biochem. J. **405:** 199–221.

Grabarek, Z. (2006). Structural basis for diversity of the EF-hand calcium-binding proteins. J. Mol. Biol. **359:** 509–525.

Gu, F., and Nielsen, E. (2013). Targeting and regulation of cell wall synthesis during tip growth in plants. J. Integr. Plant Biol. **55:** 835–846.

Gu, Y., Fu, Y., Dowd, P., Li, S., Vernoud, V., Gilroy, S., and Yang, Z. (2005). A Rho family GTPase controls actin dynamics and tip growth via two counteracting downstream pathways in pollen tubes. J. Cell Biol. **169:** 127–138.

Haruta, M., Sabat, G., Stecker, K., Minkoff, B.B., and Sussman, M.R. (2014). A peptide hormone and its receptor protein kinase regulate plant cell expansion. Science **343:** 408–411.

Hepler, P.K., Kunkel, J.G., Rounds, C.M., and Winship, L.J. (2012). Calcium entry into pollen tubes. Trends Plant Sci. **17:** 32–38.

Iwano, M., Entani, T., Shiba, H., Kakita, M., Nagai, T., Mizuno, H., Miyawaki, A., Shoji, T., Kubo, K., Isogai, A., and Takayama, S. (2009). Fine-tuning of the cytoplasmic Ca^{2+} concentration is essential for pollen tube growth. Plant Physiol. **150:** 1322–1334.

Iwano, M., Shiba, H., Miwa, T., Che, F.S., Takayama, S., Nagai, T., Miyawaki, A., and Isogai, A. (2004). Ca^{2+} dynamics in a pollen grain and papilla cell during pollination of Arabidopsis. Plant Physiol. **136:** 3562–3571.

Jones, M.A., Raymond, M.J., Yang, Z., and Smirnoff, N. (2007). NADPH oxidase-dependent reactive oxygen species formation required for root hair growth depends on ROP GTPase. J. Exp. Bot. **58:** 1261–1270.

Kawarazaki, T., Kimura, S., Iizuka, A., Hanamata, S., Nibori, H., Michikawa, M., Imai, A., Abe, M., Kaya, H., and Kuchitsu, K. (2013). A low temperature-inducible protein AtSRC2 enhances the ROS-producing activity of NADPH oxidase AtRbohF. Biochim. Biophys. Acta **1833:** 2775–2780.

Keller, T., Damude, H.G., Werner, D., Doerner, P., Dixon, R.A., and Lamb, C. (1998). A plant homolog of the neutrophil NADPH oxidase gp91phox subunit gene encodes a plasma membrane protein with Ca^{2+} binding motifs. Plant Cell **10:** 255–266.

Kimura, S., Kawarazaki, T., Nibori, H., Michikawa, M., Imai, A., Kaya, H., and Kuchitsu, K. (2013). The CBL-interacting protein kinase CIPK26 is a novel interactor of Arabidopsis NADPH oxidase AtRbohF that negatively modulates its ROS-producing activity in a heterologous expression system. J. Biochem. **153:** 191–195.

Kimura, S., Kaya, H., Kawarazaki, T., Hiraoka, G., Senzaki, E., Michikawa, M., and Kuchitsu, K. (2012). Protein phosphorylation is a prerequisite for the Ca^{2+}-dependent activation of Arabidopsis NADPH oxidases and may function as a trigger for the positive feedback regulation of Ca^{2+} and reactive oxygen species. Biochim. Biophys. Acta **1823:** 398–405.

Konrad, K.R., Wudick, M.M., and Feijó, J.A. (2011). Calcium regulation of tip growth: New genes for old mechanisms. Curr. Opin. Plant Biol. **14:** 721–730.

Kuchitsu, K., Kosaka, H., Shiga, T., and Shibuya, N. (1995). EPR evidence for generation of hydroxyl radical triggered by *N*-acetylchitooligosaccharide elicitor and a protein phosphatase inhibitor in suspension-cultured rice cells. Protoplasma **188:** 138–142.

Kwak, J.M., Mori, I.C., Pei, Z.M., Leonhardt, N., Torres, M.A., Dangl, J.L., Bloom, R.E., Bodde, S., Jones, J.D., and Schroeder, J.I. (2003). NADPH oxidase AtrbohD and AtrbohF genes function in ROS-dependent ABA signaling in Arabidopsis. EMBO J. **22:** 2623–2633.

Lee, Y., Rubio, M.C., Alassimone, J., and Geldner, N. (2013). A mechanism for localized lignin deposition in the endodermis. Cell **153:** 402–412.

Li, H., Lin, Y., Heath, R.M., Zhu, M.X., and Yang, Z. (1999). Control of pollen tube tip growth by a Rop GTPase-dependent pathway that leads to tip-localized calcium influx. Plant Cell **11:** 1731–1742.

Lin, Y., Wang, Y., Zhu, J.K., and Yang, Z. (1996). Localization of a Rho GTPase implies a role in tip growth and movement of the generative cell in pollen tubes. Plant Cell **8:** 293–303.

Liszkay, A., van der Zalm, E., and Schopfer, P. (2004). Production of reactive oxygen intermediates ($O_2^{\cdot-}$, H_2O_2, and $\cdot OH$) by maize roots and their role in wall loosening and elongation growth. Plant Physiol. **136:** 3114–3123.

Marino, D., Dunand, C., Puppo, A., and Pauly, N. (2012). A burst of plant NADPH oxidases. Trends Plant Sci. **17:** 9–15.

Messerli, M.A., Créton, R., Jaffe, L.F., and Robinson, K.R. (2000). Periodic increases in elongation rate precede increases in cytosolic Ca^{2+} during pollen tube growth. Dev. Biol. **222:** 84–98.

Michard, E., Lima, P.T., Borges, F., Silva, A.C., Portes, M.T., Carvalho, J.E., Gilliham, M., Liu, L.H., Obermeyer, G., and Feijó, J.A. (2011). Glutamate receptor-like genes form Ca^{2+} channels in pollen tubes and are regulated by pistil D-serine. Science **332:** 434–437.

Miyazaki, S., Murata, T., Sakurai-Ozato, N., Kubo, M., Demura, T., Fukuda, H., and Hasebe, M. (2009). ANXUR1 and 2, sister genes to FERONIA/SIRENE, are male factors for coordinated fertilization. Curr. Biol. **19:** 1327–1331.

Müller, K., Carstens, A.C., Linkies, A., Torres, M.A., and Leubner-Metzger, G. (2009). The NADPH-oxidase AtrbohB plays a role in Arabidopsis seed after-ripening. New Phytol. **184:** 885–897.

O'Brien, J.A., Daudi, A., Butt, V.S., and Bolwell, G.P. (2012). Reactive oxygen species and their role in plant defence and cell wall metabolism. Planta **236:** 765–779.

Oda, T., Hashimoto, H., Kuwabara, N., Akashi, S., Hayashi, K., Kojima, C., Wong, H.L., Kawasaki, T., Shimamoto, K., Sato, M., and Shimizu, T. (2010). Structure of the N-terminal regulatory domain of a plant NADPH oxidase and its functional implications. J. Biol. Chem. **285:** 1435–1445.

Ogasawara, Y., et al. (2008). Synergistic activation of the Arabidopsis NADPH oxidase AtrbohD by Ca^{2+} and phosphorylation. J. Biol. Chem. **283:** 8885–8892.

Pina, C., Pinto, F., Feijó, J.A., and Becker, J.D. (2005). Gene family analysis of the Arabidopsis pollen transcriptome reveals biological implications for cell growth, division control, and gene expression regulation. Plant Physiol. **138:** 744–756.

Potocký, M., Jones, M.A., Bezvoda, R., Smirnoff, N., and Zárský, V. (2007). Reactive oxygen species produced by NADPH oxidase are involved in pollen tube growth. New Phytol. **174:** 742–751.

Potocký, M., Pejchar, P., Gutkowska, M., Jiménez-Quesada, M.J., Potocká, A., Alché, J.D., Kost, B., and Žárský, V. (2012). NADPH oxidase activity in pollen tubes is affected by calcium ions, signaling phospholipids and Rac/Rop GTPases. J. Plant Physiol. **169:** 1654–1663.

Qin, Y., and Yang, Z. (2011). Rapid tip growth: Insights from pollen tubes. Semin. Cell Dev. Biol. **22:** 816–824.

Rodríguez, A.A., Grunberg, K.A., and Taleisnik, E.L. (2002). Reactive oxygen species in the elongation zone of maize leaves are necessary for leaf extension. Plant Physiol. **129:** 1627–1632.

Schiøtt, M., Romanowsky, S.M., Baekgaard, L., Jakobsen, M.K., Palmgren, M.G., and Harper, J.F. (2004). A plant plasma membrane Ca^{2+} pump is required for normal pollen tube growth and fertilization. Proc. Natl. Acad. Sci. USA **101:** 9502–9507.

Schmid, M., Davison, T.S., Henz, S.R., Pape, U.J., Demar, M., Vingron, M., Schölkopf, B., Weigel, D., and Lohmann, J.U. (2005). A gene expression map of *Arabidopsis thaliana* development. Nat. Genet. **37:** 501–506.

Schopfer, P. (2001). Hydroxyl radical-induced cell-wall loosening in vitro and in vivo: Implications for the control of elongation growth. Plant J. **28:** 679–688.

Sirichandra, C., Gu, D., Hu, H.C., Davanture, M., Lee, S., Djaoui, M., Valot, B., Zivy, M., Leung, J., Merlot, S., and Kwak, J.M. (2009). Phosphorylation of the Arabidopsis AtrbohF NADPH oxidase by OST1 protein kinase. FEBS Lett. **583:** 2982–2986.

Steinhorst, L., and Kudla, J. (2013). Calcium—A central regulator of pollen germination and tube growth. Biochim. Biophys. Acta **1833:** 1573–1581.

Suzuki, N., Miller, G., Morales, J., Shulaev, V., Torres, M.A., and Mittler, R. (2011). Respiratory burst oxidases: The engines of ROS signaling. Curr. Opin. Plant Biol. **14:** 691–699.

Takahashi, S., Kimura, S., Kaya, H., Iizuka, A., Wong, H.L., Shimamoto, K., and Kuchitsu, K. (2012). Reactive oxygen species production and activation mechanism of the rice NADPH oxidase OsRbohB. J. Biochem. **152:** 37–43.

Takeda, S., Gapper, C., Kaya, H., Bell, E., Kuchitsu, K., and Dolan, L. (2008). Local positive feedback regulation determines cell shape in root hair cells. Science **319:** 1241–1244.

Takemoto, D., Kamakura, S., Saikia, S., Becker, Y., Wrenn, R., Tanaka, A., Sumimoto, H., and Scott, B. (2011). Polarity proteins Bem1 and Cdc24 are components of the filamentous fungal NADPH oxidase complex. Proc. Natl. Acad. Sci. USA **108:** 2861–2866.

Torres, M.A., and Dangl, J.L. (2005). Functions of the respiratory burst oxidase in biotic interactions, abiotic stress and development. Curr. Opin. Plant Biol. **8:** 397–403.

Torres, M.A., Dangl, J.L., and Jones, J.D. (2002). Arabidopsis gp91phox homologues AtrbohD and AtrbohF are required for accumulation of reactive oxygen intermediates in the plant defense response. Proc. Natl. Acad. Sci. USA **99:** 517–522.

Wilkins, K.A., Bancroft, J., Bosch, M., Ings, J., Smirnoff, N., and Franklin-Tong, V.E. (2011). Reactive oxygen species and nitric oxide mediate actin reorganization and programmed cell death in the self-incompatibility response of *Papaver*. Plant Physiol. **156:** 404–416.

Winter, D., Vinegar, B., Nahal, H., Ammar, R., Wilson, G.V., and Provart, N.J. (2007). An "Electronic Fluorescent Pictograph" browser for exploring and analyzing large-scale biological data sets. PLoS ONE **2:** e718.

Wong, H.L., Pinontoan, R., Hayashi, K., Tabata, R., Yaeno, T., Hasegawa, K., Kojima, C., Yoshioka, H., Iba, K., Kawasaki, T., and Shimamoto, K. (2007). Regulation of rice NADPH oxidase by binding of Rac GTPase to its N-terminal extension. Plant Cell **19:** 4022–4034.

Wu, J., Shang, Z., Wu, J., Jiang, X., Moschou, P.N., Sun, W., Roubelakis-Angelakis, K.A., and Zhang, S. (2010). Spermidine oxidase-derived H_2O_2 regulates pollen plasma membrane hyperpolarization-activated Ca^{2+}-permeable channels and pollen tube growth. Plant J. **63:** 1042–1053.

Zhou, L., Fu, Y., and Yang, Z. (2009). A genome-wide functional characterization of Arabidopsis regulatory calcium sensors in pollen tubes. J. Integr. Plant Biol. **51:** 751–761.